

# Transient Heat Pipe Response and Rewetting Behavior

J.H. Ambrose\* and L.C. Chow†

*University of Kentucky, Lexington, Kentucky*

and

J.E. Beam‡

*Air Force Aero Propulsion Laboratory, Wright-Patterson Air Force Base, Ohio*

This paper describes the results of an investigation of pulsed heat pipe startup. Two types of pulsed startup of a copper/water heat pipe are examined. In the first, the mean temperature of the transport section is nearly constant with time. In the second, the entire heat pipe is increasing in temperature, so thermal energy storage in the heat pipe is significant. Dryout of the wick at the evaporator is found to occur only for heat transport rates greater than the capillary limit. A transient heat pipe model is used to explain the dryout and rewetting of the wick in the second type of pulsed startup.

## Nomenclature

|             |  |
|-------------|--|
| $A$         | = area                                     |
| $C$         | = effective heat capacity                  |
| $d$         | = screen wire diameter                     |
| $d_w$       | = wick diameter                            |
| $g$         | = gravitational constant                   |
| $h$         | = convective heat transfer coefficient     |
| $k_{hp}$    | = effective heat pipe thermal conductivity |
| $K$         | = wick permeability                        |
| $L$         | = length                                   |
| $\dot{m}_v$ | = vapor mass flow rate                     |
| $N$         | = screen mesh number                       |
| $P_m$       | = available pumping head                   |
| $Q$         | = heat transfer rate                       |
| $t$         | = time                                     |
| $T$         | = temperature                              |
| $U$         | = bulk velocity                            |
| $x$         | = position coordinate                      |
| $\alpha$    | = inverse time constant                    |
| $\epsilon$  | = wick porosity                            |
| $\lambda$   | = latent heat of vaporization              |
| $\mu$       | = dynamic liquid viscosity                 |
| $\rho$      | = liquid density                           |
| $\sigma$    | = surface tension                          |
| $\theta$    | = temperature difference                   |

## Subscripts

|          |                               |
|----------|-------------------------------|
| $c$      | = condenser section           |
| $e$      | = evaporator section          |
| $eff$    | = effective                   |
| $H$      | = heater                      |
| $max$    | = maximum capillary transport |
| $t$      | = transport section           |
| $T$      | = entire heat pipe            |
| $w$      | = wick cross section          |
| $\infty$ | = ambient                     |

## Introduction

MUCH of the previous heat pipe literature has focused on the steady-state operation of heat pipes and design modifications for improved performance. Quasi-steady-state testing techniques, where a heat pipe is subjected to a series of small step increases in power input with sufficient time between steps to reach steady-state operation, are prevalent. Such elaborate heat load histories may be impractical or impossible in many applications.

In recent years, the subject of transient heat pipe behavior has received considerable attention.<sup>1-7</sup> The prediction of heat pipe behavior when subjected to pulsed loading or transient heat loads has become an important research area. Several key questions in this area have yet to be fully answered and will require further study. The most obvious of these questions are 1) will a heat pipe achieve normal operation after a suddenly applied load, and if so, how large may this load be? and 2) if there is a dryout of the wick as a result of a pulsed heat load, under what circumstances will the heat pipe regain isothermal operation?

These are just two of the questions that require answers before the transient response of heat pipes can be fully understood. In the present investigation, these questions are studied and a simple theoretical model is used to explain the phenomenon exhibited during the pulsed startup of a screen wick water heat pipe.

## Pulsed Heat Pipe Startup

When a heat pipe is subjected to a sudden pulse of heat, the transient response will depend on the heat pipe geometry, working fluid, heat input rate, cooling rate, and effective heat capacity of the heat pipe. Consider the case of a heat pipe with convective cooling at the condenser. During steady-state operation, all energy input at the evaporator is transported by vapor and rejected at the condenser as depicted in Fig. 1a. During a pulsed startup (Fig. 1b), a portion of the energy addition at the evaporator is stored in the evaporator section. The remainder is used to vaporize the working fluid. The energy stored in the vapor is transported to the condenser and transport sections and part of it is used to heat up these two sections through condensation. The rest is rejected to the ambient. Both condenser and transport sections thus act as heat sinks, and this decreases the effective liquid return path to the evaporator (the average distance liquid must be pumped). If no dryout occurs, the heat pipe temperature will eventually reach a steady-state value sufficiently larger than the ambient fluid temperature to allow the rejection of the entire heat input

Received April 11, 1986; revision received Aug. 4, 1986. This paper is declared a work of the U.S. Government and is not subject to copyright protection in the United States.

\*Research Assistant, Mechanical Engineering.

†Associate Professor, Mechanical Engineering. Member AIAA.

‡Engineer, Power Technology Branch. Member AIAA.

rate. The energy transported by the vapor flow from the evaporator to the rest of the heat pipe will henceforth be referred to as the heat transport rate. Except during steady-state operation, this is not the same as the heat input rate. During startup, the temperature, heat transport rate, heat rejection rate, and thermal storage rate will all be changing with time.

Heat transport limit curves for the water heat pipe used in this study are shown in Fig. 2. For screen-wicked water heat pipes, the viscous, sonic, and entrainment limits typically have much larger values than the capillary limit, even for temperatures only slightly above 0°C. The viscous, sonic, and entrainment limits depend on the vapor density. Water has sufficiently high vapor density that these heat transport limitations are not usually encountered in screen wick heat pipes unless extremely small vapor flow passages are used. For this reason the capillary limit is the only heat transport limit considered in this study. Below 150°C, the capillary limit increases with temperature due to the increase in the liquid transport factor.<sup>8</sup>

Two previous investigations of transient heat pipe behavior have concluded that the capillary flow in a screen wick can respond very quickly to an induced pressure gradient and thus exhibits a quasi-steady-state behavior.<sup>1,2</sup> This means that a heat pipe with a screen wick should accommodate a pulsed heat load as large as the maximum capillary heat transport rate without dryout.

Pulsed startup refers to a step increase in power input from zero to some constant magnitude. The curves in Fig. 3 represent two possible operating conditions (the heat transport rate due to vaporization vs the transport section temperature) during a pulsed startup. These curves rise steeply and then level off because the thermal energy storage rate is initially large, but the heat transport rate increases quickly until it approaches the steady-state condition. If the heat transport rate associated with a pulsed startup is less than the capillary limit during the entire response period, no dryout will occur. This

situation is represented by line AB. For a given constant pulse magnitude, the heat transport rate may initially exceed the maximum capillary transport capability. As the temperature increases, the capillary transport capability may increase above the heat transport rate. This case is shown by line AC in Fig. 3. If this situation occurs, the wick in the evaporator will dry out partially, followed by rewetting when the capillary transport capability increases above the heat transport rate.

## Experimental Investigation

### Experimental Setup

To examine the transient phenomena exhibited during pulsed startup, tests were performed utilizing a simple screen-wicked copper/water heat pipe. The heat pipe shell was 45.72 cm (18 in.) in length, with a 2.22-cm (7/8-in.) inner diameter and a 0.165-cm (0.065-in.) wall thickness. The wick is formed from four layers of 100-mesh copper screen which were wrapped on a mandrel and inserted into the shell so as to conform to the inner diameter.

Heat input to the pipe was provided by an Inconel sheathed nichrome heater wire coiled around the 10.16-cm (4-in.) long evaporator section. Electrical power input to the heater was provided by a regulated dc power supply. Forced air cooling was supplied by a squirrel-cage fan. The experimental apparatus is shown in Fig. 4. Wall temperatures were measured with copper-constantan thermocouples at eight locations. Wall temperatures, the ambient air temperature, and the

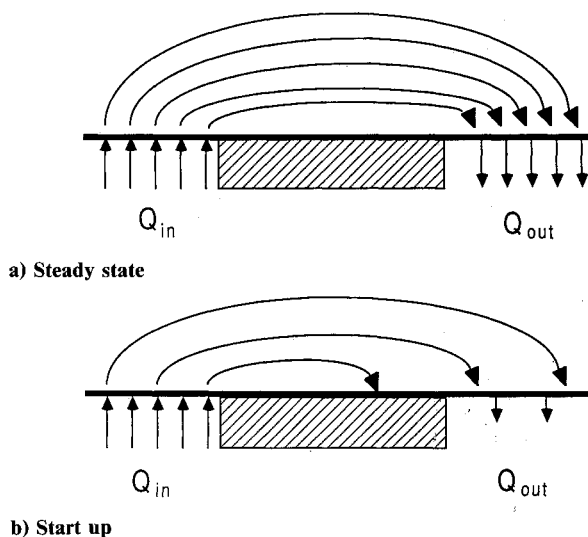


Fig. 1 Heat transport by vapor.

Table 1 Model input parameters

| Constants                                    | Dimensions                          |
|--|-------------------------------------|
| $\alpha = 2.55(10^{-3}) \text{ s}^{-1}$      | $A_w = 5.75(10^{-5}) \text{ m}^2$   |
| $h = 200 \text{ W/m}^2 \cdot ^\circ\text{C}$ | $A_c = 7.13(10^{-3}) \text{ m}^2$   |
| $K = 1.93(10^{-10}) \text{ m}^2$             | $L_{\text{eff}} = 35.56 \text{ cm}$ |
| $C_e = 109 \text{ J/}^\circ\text{C}$         | $L_c = 10.16 \text{ cm}$            |
|  | $L_e = 10.16 \text{ cm}$            |
|  | $d_w = 2 \text{ cm}$                |
|  | $N = 100 \text{ in.}^{-1}$          |

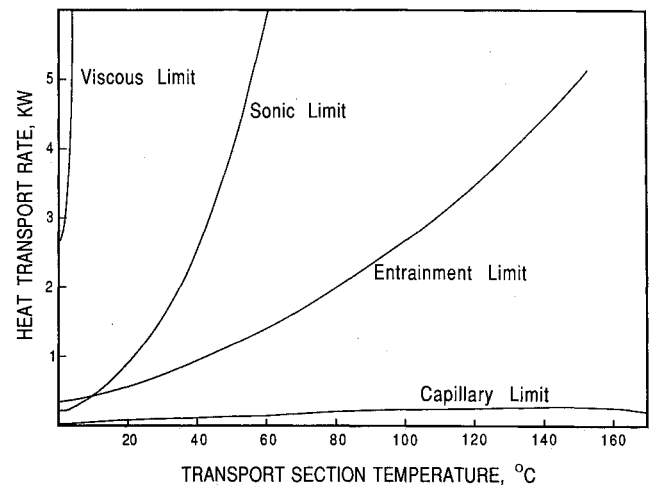


Fig. 2 Heat pipe operating limits.

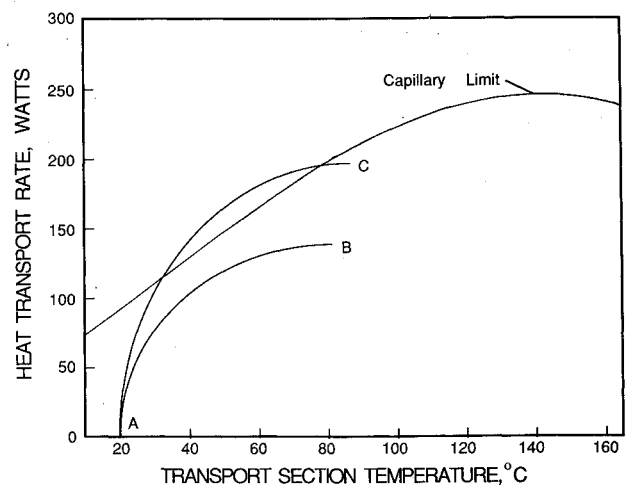


Fig. 3 Heat pipe startup.

power input rate to the heater were monitored and recorded with a data logger.

The two types of pulsed startup tests performed were those with and without thermal energy storage in the heat pipe. For those tests with thermal energy storage, the condenser section was 10.16 cm (4 in.) in length. For those tests without thermal energy storage, the condenser section was 20.32 cm (8 in.) in length.

Heat losses from the apparatus were reduced by wrapping the heater and transport sections with ~6 cm of ceramic fiber insulation and three layers of foil radiation shielding. Heat losses were estimated at less than 10% of the power input to the heater.

#### Experimental Verification of Capillary Limit

The capillary limit for the water heat pipe used in this study is shown in Fig. 5. This curve is calculated by the following equation from Chi<sup>9</sup> for a 20.32-cm condenser;

$$Q_{\max} = \frac{4\sigma N - \rho g d_w}{F_t L_{\text{eff}}}$$

where

$$F_t = \frac{\mu_l}{KA_w \rho \lambda}$$

for the case of laminar liquid flow. The experimental verification of this curve was performed by moving the operating point across the curve at several temperatures by one of three methods. Either the cooling level was increased or decreased while maintaining a constant power input (line AB, Fig. 5), or the power input was increased while maintaining a constant temperature in the transport section (line CD). Points indicating normal operation correspond with steady-state data. The dashed lines connecting normal operation and dryout points are used only to relate the two points and do not indicate an actual series of operating conditions. Dryout of the evaporator wick was observed as an abnormal increase in the temperature in the evaporator. As is seen by the points indicating dryout in Fig. 5, the capillary limit curve is reasonably accurate.

#### Pulsed Startup with Thermal Storage

When the heat pipe temperature changes significantly during the pulsed startup, a drying of the wick may occur temporarily, followed by rewetting. For these tests, a sudden power input was applied to the heat pipe when it was initially in thermal equilibrium with the ambient and sustained until the pipe was near a steady-state temperature. Typical transient temperature profiles are shown in Figs. 6 and 7 for two power levels, 125 and 225 W, respectively. At 125 W the heat transport rate remains below the capillary heat transport limit for the entire response period. The heat pipe can transport the heat load without dryout. This is indicated by the absence of large temperature gradients in the evaporator. However, at 225 W the heat transport rate temporarily exceeds the capillary heat transport limit and a partial dryout occurs. A large

temperature gradient exists across the evaporator at 200 s. The rewetting of the wick is exhibited as a decrease in the temperature gradient at 500 s.

The drying and rewetting of the wick is also shown in Fig. 8 for two heat input rates. Outside evaporator and inside evaporator refer to temperatures measured by thermocouples 1 and 2, respectively (see Fig. 4). When the outside temperature increases more quickly than the rest of the heat pipe, it is because this region is partially dry. Without liquid supply in the region, the local evaporative heat transfer is reduced. The reduction in heat transfer requires that some of the additional thermal energy be stored, which raises the temperature in the region. It is seen that the magnitude of the dryout increases with heat flux. This is caused by an increase

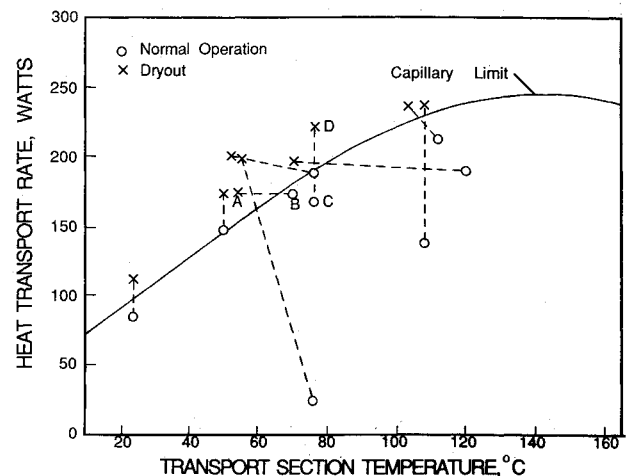


Fig. 5 Verification of capillary limit.

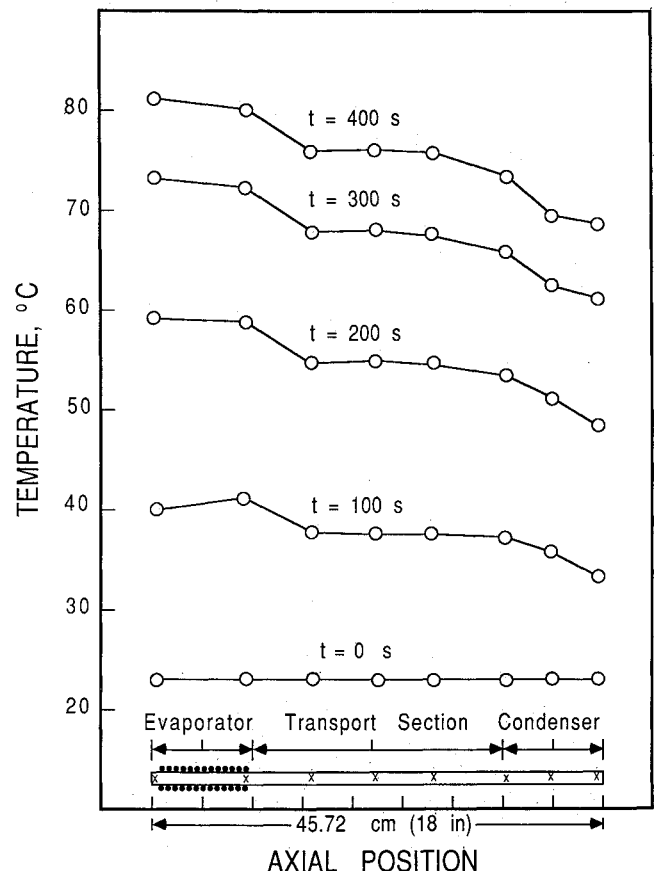


Fig. 6 Transient temperature profiles ( $Q_{\text{in}} = 125$  W).

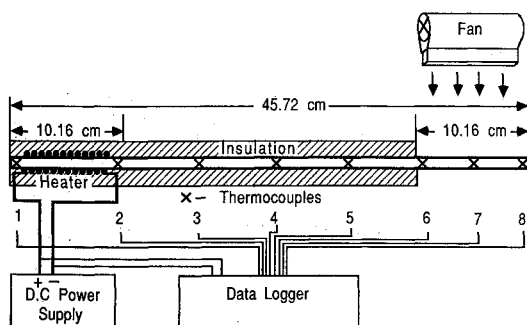


Fig. 4 Experimental apparatus.

in the size of the dried region and/or an increase in the thermal energy storage in the dry region.

#### Pulsed Startup without Thermal Storage

Pulsed startup tests with negligible thermal storage were performed to verify that the liquid flow in a screen wick can respond quickly to a change in the pressure gradient. Without thermal storage, the heat pipe must immediately transport the entire heat load to the condenser. If the transport limit is exceeded, the wick will not rewet itself but will continue to dry out as long as the power input is maintained.

Pulsed startup without thermal storage was accomplished by applying a sudden power input to the heat pipe via the electric resistance heater and varying the cooling rate so that the transport section remained at the same temperature. For these tests, the condenser section was 20.32 cm (8 in.) in length to accommodate a radiant heater used only to raise the heat pipe temperature uniformly prior to a test. The tests were conducted at four different initial temperatures. At each temperature, power inputs above and below the capillary limit were applied.

For tests performed at room temperature, the radiant heater was not used, and cooling was accomplished by a combination of forced air and cold water drip. The drip rate was increased gradually to maintain the transport section at room temperature. For the elevated temperature runs, the condenser of the heat pipe was surrounded by a clamshell-type radiant heater so that the entire pipe could be heated uniformly. When the heat pipe was isothermal at the desired elevated temperature, the clamshell heater was quickly removed. The desired pulse load was applied at the evaporator and the condenser was cooled by forced air. The cooling level was varied by changing the distance of the fan from the condenser.

Dryout was observed only for those pulses that exceeded the predicted capillary limit to heat transport at the given pulse temperature. The tests verify that the liquid flow can respond quickly to a change in the pressure gradient.

#### Analytical Model

##### Transient Temperature Response

Beam<sup>1</sup> developed a lumped parameter model from an energy balance on the entire heat pipe. Since the effective thermal conductivity of the heat pipe is very large, the Biot number ( $hL_T/k_{hp}$ ) is small and the lumped parameter approach is justified. An energy balance for the entire heat pipe gives

$$Q_{in} = Q_{out} + Q_{stored} \quad (1)$$

If the heat pipe is cooled by convection to an ambient fluid (transport section insulated), the energy balance becomes

$$Q_{in} = hA_c\theta + C_T \frac{d\theta}{dt} \quad (2)$$

where  $\theta = T - T_\infty$ . The heat transfer coefficient for the case of forced air cooling is only weakly dependent on the temperature. The variation of the effective heat capacity with temperature was calculated and is negligible. The solution to Eq. (2) is

$$\theta = \theta_o e^{-\alpha t} + \frac{Q_{in}}{hA_c} [1 - e^{-\alpha t}]$$

where  $\theta = \theta_o = T_o - T_\infty$  at  $t = 0$  and

$$\alpha^{-1} = \frac{C_T}{hA_c}$$

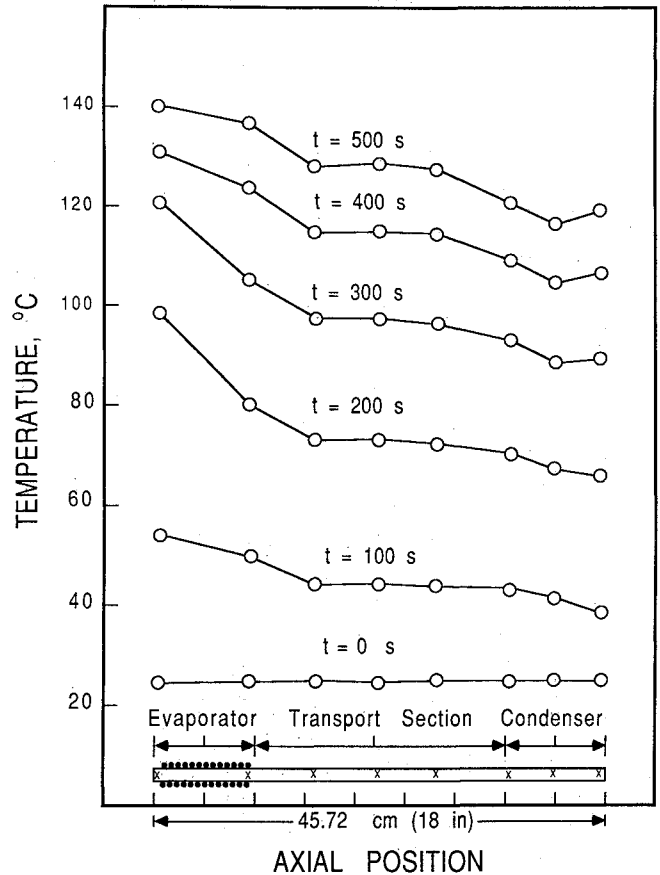


Fig. 7 Transient temperature profiles ( $Q_{in} = 225$  W).

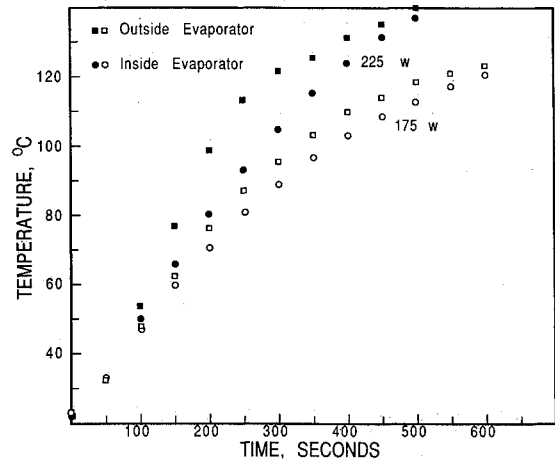


Fig. 8 Pulsed startup with thermal storage.

is the time constant. This is simplified to

$$\theta = \frac{Q_{in}}{hA_c} [1 - e^{-\alpha t}] \quad (3)$$

for  $\theta_o = 0$ , when the pipe is initially in equilibrium with the surroundings.

The values of the time constant and the heat transfer coefficient are determined experimentally for a given heat pipe and cooling condition. At a steady state, the energy storage term becomes zero and Eq. (2) becomes

$$Q_{in} = hA_c\theta$$

Thus the heat transfer coefficient can be measured from the heat input and average temperature. During a pulsed startup, the average temperature is measured as a function of time and the inverse time constant  $\alpha$  is the slope of the curve of

$$\ln \left[ \frac{Q_{in}}{Q_{in} - hA_c \theta} \right] = \alpha t \tag{4}$$

Equation (4) is plotted from experimental pulsed startup data in Fig. 9. The graph indicates that during the first 45 s of the pulse period there is a significant thermal lag. The thermal lag occurs because the electric heater must be heated up before it can supply heat to the heat pipe. Early in the pulse period, the heater absorbs most of the energy input. Given the measured heat capacity of the heater  $C_H = 105 \text{ J/}^\circ\text{C}$ , it can be shown that, for the range of heat input considered, the thermal lag is of the order of 50 s.

The transient temperature response, Eq. (3), has been modified slightly to account for the thermal lag. The thermal lag is characterized by the intercept of the line in Fig. 9 at  $t = 0$ . If the thermal lag is accounted for, then the temperature response becomes

$$\theta = \frac{Q_{in}}{hA_c} \left[ 1 - e^{-\alpha t + 0.08} \right]$$

For  $t$  less than 45 s, this solution has a much larger slope than the measured data, as shown in Fig. 10. This is corrected by approximating the temperature for  $t < 45$  s by a linear profile (dotted line, Fig. 10). The reduced rate of energy storage in the heat pipe during the initial pulse period is expected because of the additional energy storage required by the heater. The modified, transient temperature response is then

$$\begin{aligned} \theta &= \frac{\theta(45)}{45} t & t \leq 45 \text{ s} \\ \theta &= \frac{Q_{in}}{hA_c} \left[ 1 - e^{-\alpha t + 0.08} \right] & t > 45 \text{ s} \end{aligned} \tag{5}$$

Transient Liquid Model

Beam<sup>1</sup> modeled the dryout of the wick at the evaporator by assuming a distinct interface to exist between completely dry and completely saturated regions. The interface is perpendicular to the liquid flow direction and serves as a moving boundary of the control volume, as shown in Fig. 11. This simplified model is used in the present investigation to model the drying and rewetting of the wick during a pulsed startup with thermal storage. Experimental measurements of the liquid saturation in heat pipe wicks made by Shishido and Ohtani<sup>10</sup> indicate that the liquid front model is a good approximation. Their data shows that at higher heat loads, the liquid saturation is nearly unity along the condenser and transport sections and drops sharply in the evaporator section.

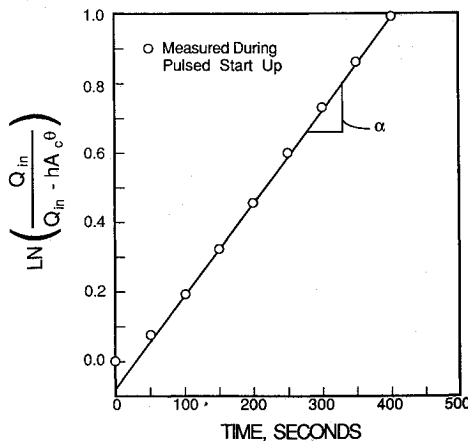


Fig. 9 Determination of time constant.

The movement of the liquid/vapor interface shown in Fig. 11 is governed by the continuity of the mass flow entering (liquid) and leaving (vapor) the control volume. If the liquid enters from the right in the positive  $x$  direction with velocity  $U$ , the conservation of mass of the liquid requires that

$$\rho A_w U = \rho A_w \frac{dx}{dt} + \dot{m}_v \tag{6}$$

The flow within the wick is slow and Darcy's Law is assumed to be valid;

$$U = \frac{P_m K}{\mu (x - x_o)}$$

where

$$P_m = 4\sigma N - \rho g d_w$$

$$x_o = \frac{L_e + L_c}{2}$$

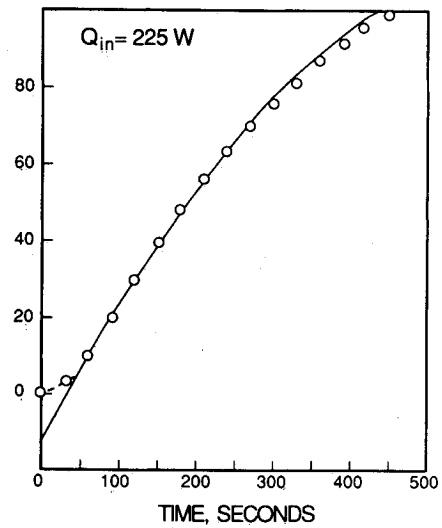


Fig. 10 Lumped model prediction.

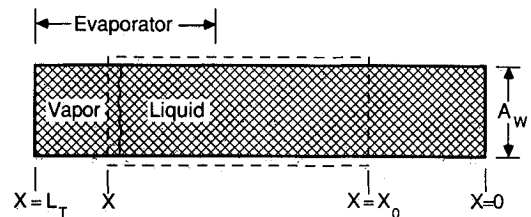


Fig. 11 Wick control volume.

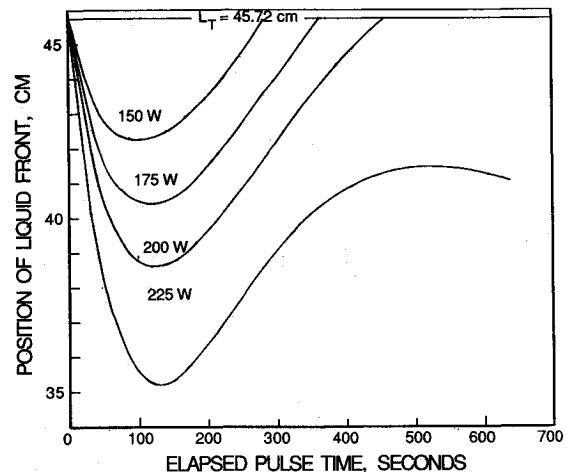


Fig. 12 Movement of liquid front.

The permeability  $K$  is estimated from a modified Blake-Kozeny equation,<sup>9</sup>

$$K = \frac{d^2 \epsilon^3}{122(1-\epsilon)^2}$$

Here  $x - x_0$  represents an equivalent pumping length. This is consistent with the calculation of the capillary limitation to heat transport based on the effective length for the liquid return

$$L_{\text{eff}} = L_t + \frac{L_e + L_c}{2}$$

For a given value of  $x$ , the maximum capillary pumping head is assumed. This assumption is made because of the nature of the simplified model. If a distinct interface exists within the wick (rather than at the surface), then the minimum pumping radius of the wicking material would likely exist at this interface.

Because of the thermal storage, the vapor mass flow rate  $\dot{m}_v$  in Eq. (6) will vary with time. The temperature profiles in Figs. 6 and 7 show that the axial conduction along the shell and wick is small. Thus the energy stored in the transport and condenser sections of the heat pipe must be supplied by vapor condensation. An energy balance on the evaporator section yields

$$Q_{\text{in}} = C_e \frac{d\theta}{dt} + \dot{m}_v \lambda$$

where the last term is due solely to evaporation and the heat capacity  $C_e$  is the fraction of the total heat capacity attributed to the evaporator section. This equation is combined with Eq. (5) to define the mass flow of vapor as

$$\dot{m}_v = \frac{1}{\lambda} \left[ Q_{\text{in}} - C_e \frac{\theta(45)}{45} \right] \quad t \leq 45 \text{ s} \quad (7)$$

$$\dot{m}_v = \frac{Q_{\text{in}}}{\lambda} \left[ 1 - \left( \frac{C_e}{C_T} \right) e^{-\alpha t + 0.08} \right] \quad t > 45 \text{ s}$$

Equations (6) and (7) describe the movement of the liquid front during a pulsed startup with thermal storage.

The solution of Eq. (6) proceeds from the starting conditions of a wick initially full of liquid and a constant heat load applied at  $t=0$ . These conditions correspond to (see Fig. 10)

$$x(t=0) = L_T, \quad Q_{\text{in}}(t \geq 0) = \text{const}$$

Equations (6) and (7) were solved by the Runge-Kutta method to obtain a solution for the position of the liquid front as a function of time. At each new time step, the mean operating temperature was evaluated from the modified transient temperature response, Eq. (5). The fluid properties were then evaluated at this temperature using least-square polynomial approximations taken from Ref. 8.

Using the experimentally determined parameters  $\alpha$  and  $h$  as described earlier, the transient liquid model Eq. (6) was solved for the case of a 45.72-cm (18-in.) long heat pipe with a four-layer 100-mesh screen wick. The value of  $h$  used in the solution corresponds to the case of forced air cooling, and the evaporator, transport, and condenser lengths are 10.16 cm (4 in.), 25.4 cm (10 in.), and 10.16 cm (4 in.), respectively. The input parameters used for the analytical model are listed in Table 1.

The behavior of the liquid front is shown in Fig. 12 for various power inputs. The liquid front recedes from its initial position, corresponding to a partial dryout of the wick. In most cases, the front reverses direction and returns to its original position, corresponding to a complete rewetting of the wick. The recession of the liquid front occurs when the rate of evaporation of liquid is greater than the maximum liquid return flow rate that the capillary pumping can supply. Reversal of the liquid front movement occurs when the capillary pumping is sufficient to supply more liquid than is depleted through evaporation.

Theoretical results as shown in Fig. 12 are similar to experimental results shown in Fig. 8. Both show a drying and rewetting of the wick due to increasing liquid return flow. Both indicate a more substantial dryout of the wick at higher heat fluxes. The time required for the wick to rewet is on the order of several hundred seconds. The rewetting time is somewhat longer in the experimental data and is nearly independent of heat flux. Theoretical results indicate that no rewetting will occur for pulses of 225 W or greater, while the experimental results show rewetting for 225 W. The one-dimensionality of the model requires that the wick begins to dry out immediately after the pulse is applied. Any depletion of liquid will cause dryout, i.e. the liquid front recedes along the wick. In the actual heat pipe, some depletion of liquid in the evaporator wick can occur without causing dryout. Increased thermal storage in the dry region of the wick is ignored in the model because only the average heat pipe temperature given by the lumped parameter solution is used in the transient liquid model. The dryout in the heat pipe will thus occur more slowly and the heat pipe will reach higher temperatures. This explains the observed rewetting of the wick at 225 W.

### Conclusions

A prediction of the transient response of a heat pipe to a pulsed startup was made. The transient response depends on the capillary pumping, the mechanism of cooling, and the heat capacity of the heat pipe. Three possible responses to a pulsed power input can occur. The wick in the evaporator may accommodate the heat input without dryout, dryout partially followed by rewetting, or dryout without rewetting. Predictions of the dryout and rewetting behavior were made using a lumped parameter model, and good agreement with experiments was shown.

Liquid in a screen wick can respond almost instantaneously to a change in the pressure gradient. This is verified by the ability of the heat pipe to transport a pulsed heat load equal to the capillary transport limit without dryout while maintaining the heat pipe at a constant temperature.

### Acknowledgments

This work was cosponsored by the Air Force Aero Propulsion Laboratory and the Air Force Office of Scientific Research. The work was performed at the Aero Propulsion Laboratory, Wright-Patterson Air Force Base, Ohio. The technical assistance provided by Mr. D. Reinmuller is gratefully acknowledged.

### References

- Beam, J.E., "Unsteady Heat Transfer in Heat Pipes," Ph.D. Dissertation, School of Engineering, University of Dayton, 1985.
- Colwell, G.T. and Chang, W.S., "Measurement of the Transient Behavior of a Capillary Structure Under Heavy Thermal Loading," *International Journal of Heat and Mass Transfer*, Vol. 27, 1984, pp. 541-551.
- Chang, W.S. and Colwell, G.T., "Mathematical Modeling of the Transient Operating Characteristics of a Low-Temperature Heat Pipe," *Numerical Heat Transfer*, Vol. 8, 1985, pp. 169-186.
- Cullimore, B.A., "Modeling of Transient Heat Pipe Effects Using a Generalized Thermal Analysis Program," AIAA Paper 85-0938, June 1985.
- Tilton, D.E., Chow, L.C., and Mahefkey, E.T., "Transient Response of a Liquid Metal Heat Pipe Subjected to External Loading at the Condenser," AIAA Paper 86-1271, June 1986.
- Merrigan, M.A., Keddy, E.S., and Sena, J.T., "Transient Performance Investigation of a Space Power System Heat Pipe," AIAA Paper 86-1273, June 1986.
- Supper, W. and Groll, M., "Heat Pipe Tests on Space Shuttle Flights," SAE Paper 851356, July 1985.
- Brennan, P.S. and Krolczek, E.J., *Heat Pipe Handbook*, Vol. 2, B&K Engineering, Inc., Towson, MD, June 1979.
- Chi, S.W., *Heat Pipe Theory and Practice*, Hemisphere Publishing Corp., Washington, D.C., 1976.
- Shishido, I. and Ohtani, S., "Working Fluid Distribution Within Heat Pipe Wick," *Proceedings of the Fifth International Heat Pipe Conference*, Tsukuba, Japan, 1984.